DALHOUSIE UNIVERSITY

Investigation of weld effective length rules for CHS X-connections

K. Tousignant & J. A. Packer
Department of Civil Engineering, University of Toronto, Toronto, Canada

ABSTRACT: A laboratory-based test program was conducted to assess the performance of fillet welds in X-connections between circular hollow sections (CHS). Six full-scale, fillet-welded CHS-to-CHS X-connections were designed to be weld-critical with varied key parameters that affect weld strength: branch-to-chord diameter ratio, chord wall slenderness, and branch inclination angle. By means of quasi-static tension applied to the ends of each branch, fracture of 12 test welds (two per connection) was obtained. Strain distributions adjacent to the weld and branch loads at rupture were measured. By using the carefully measured mechanical and geometrical properties of the fillet welds and CHS members, the structural reliability (or safety index) of the existing AWS specification provisions for weld effective lengths in CHS-to-CHS X-connections was determined. For the range of parameters studied, the existing AWS formulae were found to be very conservative, hence a comprehensive parametric modelling study is planned to develop more liberal recommendations.

1 INTRODUCTION

When welding to hollow structural sections (HSS), welds can be proportioned: (a) to achieve the capacity of the connected member walls, or (b) as "fit for purpose" (ISO 2013). By designing welds as "fit for purpose" – to resist the actual forces present in the branch member – smaller, more appropriate weld sizes typically result.

In order to account for the non-uniform loading of the weld perimeter due to differences in the relative flexibilities of the chord loaded normal to its surface, and the branch(es) carrying membrane stresses parallel to its surface, weld effective properties – including weld effective lengths and weld effective section moduli – are used. These properties are determined by discounting segments of the weld which do not contribute to its overall resistance.

Over the last 30 years, much research has been conducted at the University of Toronto to determine weld effective lengths for rectangular hollow section (RHS) connections, including gapped K-connections (Frater & Packer 1992a, 1992b), T-, Y- and X- (or Cross-) connections (Packer & Cassidy 1995), moment-loaded T-connections (McFadden & Packer 2014), and overlapped K-connections (Tousignant & Packer 2015). Recommendations based on this research have been adopted as code in North America, by the American Institute of Steel Construction (AISC) in Section K5: "Welds of Plates and Branches to RHS" of their latest (2016) specification (AISC 2016).

Since the addition of Section K5 (formerly Section K4, in the 2010 specification), weld effective properties for circular hollow section (CHS) connections have been an issue faced by code writers, including AISC and the American Welding Society (AWS), since load transfer around a welded CHS joint can be highly non-uniform (Marshall 1992).

While AISC 360-16 is noticeably silent regarding weld effective lengths for CHS connections, AWS D1.1-15 "Structural Welding Code – Steel" implies, in Clause 9.6.1.3(4), that the weld effective length in axially loaded CHS connections is equal to 1/1.5 of the total weld length under factored loads, regardless of the joint geometry. While believed to be conservative, this rule is not supported by experimental evidence.

A laboratory-based test program was hence conducted to assess the performance of welds in CHS connections. For the first time ever, weld-critical tests (where failure occurs by weld fracture) were completed on fillet welds in full-scale CHS X-connections, and the structural reliability (safety index) of the existing AWS and AISC specification provisions for the design of such welds was determined. This paper reports on the findings.

2 EXPERIMENTATION

Six CHS X-connections were designed and fabricated from ASTM A500 (ASTM 2013) dual-certified Grade B and C cold-formed CHS, and fillet welded using a semi-automatic flux-cored arc welding process with a CO_2 shielding gas. As it was speculated that the strength of welds in CHS X-connections depends on branch-to-chord diameter ratio ($\beta = D_b/D$), chord wall slenderness (D/t), and branch inclination angle (θ), the chord and branch members were selected to cover a wide range of these values (Table 1), within limits for fillet welds to develop the full throat thickness (given by AWS D1.1-15 – see Section 2.1). Four connections had branches at 90° to the chord, and two connections had branches at 60° to the chord. The connection layout is shown in Figure 1.

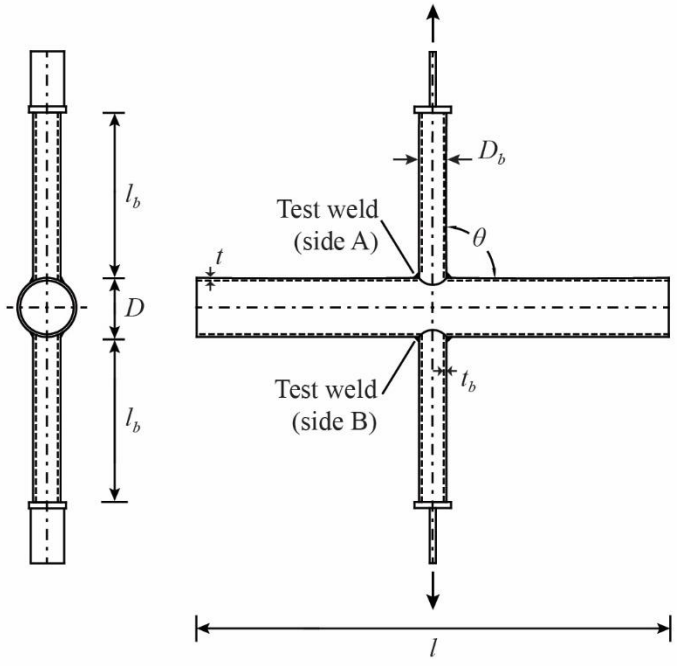

Figure 1. Connection layout.

2.1 *Connection geometric considerations*

CHS members and connection geometry had to be carefully designed, to maintain the local dihedral angle (Ψ) (Fig. 2) of the joints between 60° - 120°, to develop the full fillet weld throat thickness (t_w). According to Note [4] in AWS D1.1-15 Figure 9.10, when Ψ < 60°, the Z loss values in AWS D1.1-15 Table 9.5, for PJP welds, apply. To keep Ψ within this range, the complex effect of β and θ on Ψ, which changes continuously around the joint, was studied using a vector-calculus approach (Luyties & Post 1988). It was determined that β must not exceed 0.50 for 90° CHS connections, and 0.28 for 60° CHS X-connections. While having θ less than 60°, and thus Ψ less than 60°, would adversely affect the weld strength by contributing to the Z loss (loss of the weld throat) at the root of the weld, having slightly larger β-values, and thus Ψ slightly greater than 120° does not. It was therefore deemed necessary to keep θ between 60° and 90°, while a minor deviation from the stated β limits was considered acceptable.

The branches were cut to a minimum branch length (l_b) of $6D_b$, to avoid shear lag effects at mid-length, from both ends (Mehrota & Govil 1972), and profiled to saddle perfectly onto the chords, without edge bevelling. The chords were cut to an overall chord length (l) to avoid end effects at the connection (van der Vegte & Makino 2010). To economize material, they were left unrestrained (uncapped) at each end.

2.2 *Geometrical and Mechanical Properties of the as-laid welds*

Correct input for the geometric and mechanical properties of the welds, which comprise a complex saddle shape in CHS connections, is critical to the scientific analysis of the weld strength; hence, great lengths were taken to very accurately obtain these measurements.

After being laid, welds were angle-ground to have a near-uniform throat size (t_w) around each joint, and flat weld faces. Flat weld faces allowed t_w to be obtained from a 3D model of the weld's exact geometry, as shown in Figure 2.

Using this approach, the orientation of the weld legs (l_v and l_h) must be established correctly: in the plane of Ψ, perpendicular to the weld root, between tangents to the outside surfaces of the branch and the chord. The computer-aided design program Solidworks was employed to exact this requirement.

First, components of l_v and l_h parallel to the branch were measured at uniform subtended angle (ρ) increments along the weld length. Then, the weld profile around the entire joint was modelled (in

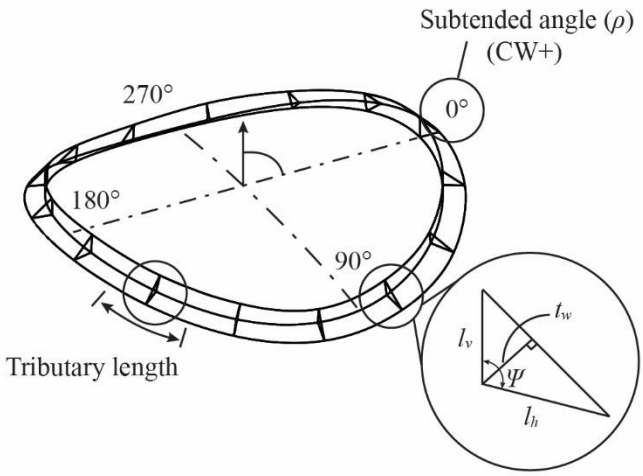

Figure 2. 3D Solidworks model of weld profile and weld dimensions.

Table 1. Measured properties of twelve CHS X- (test) connections.

Test	CHS branch member			CHS chord member			θ	β	D/t	τ	P_a***
	$D_b \times t_b$ mm × mm	A_b* mm^2	F_{yb}** MPa	$D \times t$ mm × mm	A* mm^2	F_y** MPa	°				kN
102-273-90a	102.0 × 7.34	2161	373	273.5 × 11.69	9614	460	90	0.37	23.4	0.63	672
102-273-90b	102.0 × 7.34	2161	373	273.5 × 11.69	9614	460		0.37	23.4	0.63	678
102-406-90a	102.0 × 7.34	2161	373	406.5 × 12.34	15,283	355		0.25	32.9	0.59	608
102-406-90b	102.0 × 7.34	2161	373	406.5 × 12.34	15,283	355		0.25	32.9	0.59	540
127-273-90a	127.4 × 11.55	4207	431	273.5 × 11.69	9614	460		0.47	23.4	0.99	653
127-273-90b	127.4 × 11.55	4207	431	273.5 × 11.69	9614	460		0.47	23.4	0.99	>653
127-406-90a	127.4 × 11.55	4207	431	406.5 × 12.34	15,283	355		0.31	32.9	0.94	557
127-406-90b	127.4 × 11.55	4207	431	406.5 × 12.34	15,283	355		0.31	32.9	0.94	>557
102-406-60a	102.0 × 7.34	2161	373	410.0 × 12.21	15,260	373	60	0.25	33.6	0.60	721
102-406-60b	102.0 × 7.34	2161	373	410.0 × 12.21	15,260	373		0.25	33.6	0.60	>721
127-406-60a	127.4 × 11.55	4207	431	410.0 × 12.21	15,260	373		0.31	33.6	0.95	761
127-406-60b	127.4 × 11.55	4207	431	410.0 × 12.21	15,260	373		0.31	33.6	0.95	>850

*Cross-sectional areas determined by cutting a prescribed length of CHS, weighing it, and then using a density of 7850 kg/m^3 to calculate its cross-sectional area.
**Yield strength of all CHS determined from tensile coupon tests performed according to ASTM A370 (2017).
***Force in branch member at weld fracture; > preceding P_a indicates that the specimen sustained a higher load in a previous loading cycle (e.g. testing of the weld on the opposite side) without rupture.

Solidworks) using these measurements, and measured values of D_b and D. Finally, sections were taken through the weld, in the plane of Ψ, and l_v, l_h and t_w were measured (Fig. 2).

External measurement of the components of l_v and l_h is also a complicated procedure that requires the location of the weld toes to be determined relative to the root (the branch-to-chord intersection). To verify the values of l_v and l_h obtained by external measurement, post-rupture macro-etch examinations of the fillet welds were performed after several tests. The macro-etch weld leg measurements gave credence to the external measurements, used herein.

The total weld length (l_w), and the weld length tributary to each throat size measurement (which is necessary to determine the average throat size for the joint), were calculated by modifying the vector-calculus approach to determine Ψ to give a near-perfect solution for the distance between points along the weld root, and then summing up these distances. A similar approach has previously been used to determine the angle of loading of the weld, and hence the stress components on the weld at any point along its length (Tousignant & Packer 2016).

The weld area (A_w) was determined by summing up: t_w × tributary weld length around the entire joint (weighted average); the tributary weld length is shown in Figure 2. For the weighted average, 12 or 15 divisions were used for branches with D_b = 102.0 or 127.4 mm, respectively. The measured fillet-weld geometric properties are shown in Table 2.

The mechanical properties of the as-laid welds were determined by tensile coupon testing in accordance with AWS D1.1 (AWS 2015). The average yield stress from three coupon tests (by 0.2% strain offset) was 517 MPa and the average ultimate stress (F_{EXX}) was 577 MPa with 28.1% elongation at rupture. The measured ultimate strength was 17.8%

Table 2. Weld dimensions and predicted fracture load for test joints according to existing AWS D1.1-15 provisions for weld effective lengths in CHS X-connections.

Test	Average measured weld dimensions					P_n*
	l_v mm	l_h mm	t_w mm	l_w mm	A_w mm	kN
102-273-90a	6.86	6.17	4.08	322	1312	303
102-273-90b	7.23	6.65	4.37	322	1405	324
102-406-90a	5.16	5.78	3.56	320	1139	263
102-406-90b	4.54	5.08	3.14	320	1004	232
127-273-90a	5.94	5.93	3.63	406	1475	340
127-273-90b	7.05	6.06	4.00	406	1625	375
127-406-90a	4.83	5.03	3.16	403	1273	294
127-406-90b	5.60	5.19	3.47	403	1410	323
102-406-60a	5.83	5.59	3.58	345	1235	285
102-406-60b	6.29	5.83	3.79	345	1307	302
127-406-60a	5.68	8.01	3.95	434	1716	396
127-406-60b	5.39	6.00	3.38	434	1468	339

*Nominal predicted fracture load according to the existing AWS D1.1-15 specification provisions, calculated using Equations 1, 2, and 3, using A_w and F_{EXX} determined from tensile coupon tests (= 577 MPa).

greater than the specified nominal strength (490 MPa) of the E71T-1C electrode used. The welding process specifications used for the joints were: voltage = 25 V, amperage = 260 A, and travel speed = 230 mm/min.

3 TESTING METHOD AND INSTRUMENTATION

Quasi-static axial load was applied to the end of each branch on either side of the connection, and hence to the weld, by a 2700-kN capacity universal testing machine (UTM). The testing arrangement is shown in Figure 3.

Four linear strain gauges (SGs) equally spaced around the perimeter of the branch at mid length ($\geq 3D_b$ from the welded test joint and the end), and oriented along its longitudinal axis, were used to measure the uniformity of load being applied to the branch. Seven additional SGs, with the same orientation, were used around half the weld perimeter (i.e. on one side of the branch only, due to symmetry) to measure non-uniform loading of the weld perimeter (Fig. 4). For this purpose, SGs were centred 20 mm away from the weld toe to avoid stress concentrations that occur there due to the notch effect (Packer & Cassidy 1995). A single SG in the saddle position on the opposite side was used to verify symmetry of the strain distribution about the plane of the connection.

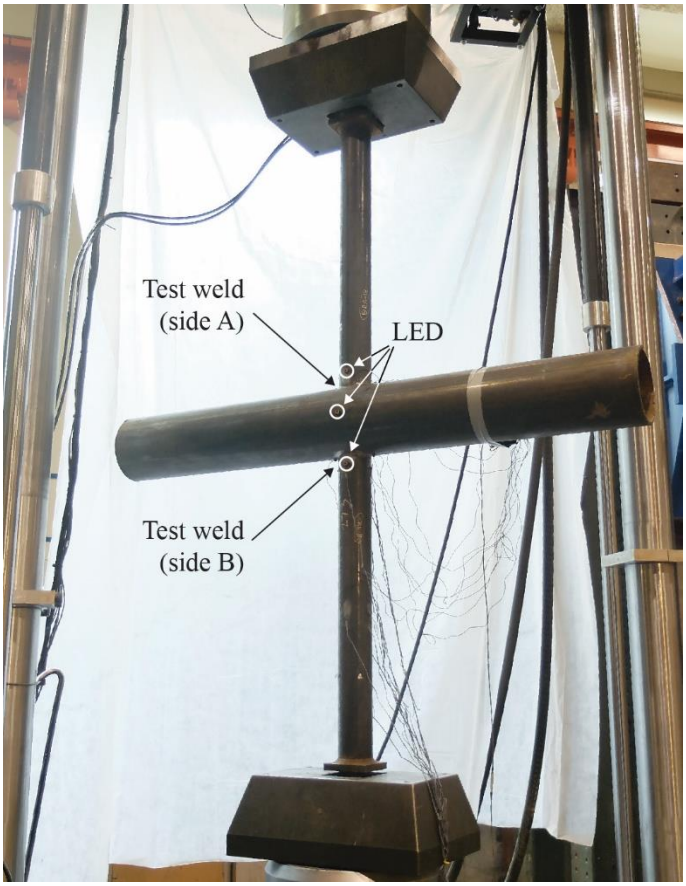

Figure 3. Testing arrangement.

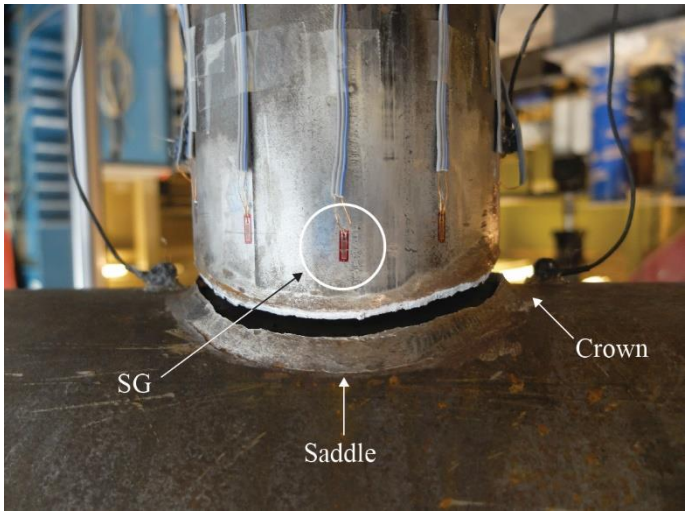

Figure 4. Strain gauges near weld toe and weld fracture in test 127-273-90a.

Figure 5. Weld fracture in test 102-406-60a

In all, 12 welds were tested to rupture (two per connection). All welds failed in a brittle manner, by fracture along a plane through the weld. A typical failure is shown in Figure 4 (for a 90° connection) and Figure 5 (for a 60° connection).

After the first test weld (e.g. Side A) ruptured in each connection, the branch was re-positioned within the UTM and tack-welded back in place. The entire connection was then removed from the UTM, and fully re-welded (nominally in the flat position) to ensure separation of the same branch did not occur again. The connection was re-placed in the UTM, and tested until rupture of the second test weld (e.g. Side B) occurred. Chord deformation (δ) was continuously monitored throughout both tests, using Metris software and an LED scanner, with three LED targets: one on each branch, 50 mm above the crown; and one at the connection work point on the chord face parallel to the plane of the connection (Fig. 3). The value of δ, which is the outward displacement (normal to the chord) of a single branch from the chord centreline (Packer et

al. 2012), was taken as half of the vertical displacement between the LEDs on each branch (Fig. 6). It therefore represents the average deformation on both sides of the connection.

The actual weld fracture loads (P_a) were obtained from load cells in-line with the UTM actuator, and verified by comparison with forces computed from average SG readings of strain at mid-length of the branch and the measured branch cross-sectional area and elastic modulus. These are given in Table 1.

4 COMMENTS ON RESULTS

Figure 6 shows the relationship between δ, expressed as a fraction of the chord diameter (δ/D), and the applied load (P) for several representative tests. Despite having only small fillet welds, it can be seen that chord plastification in excess of the 3%D deformation limit (Lu et al. 1994) occurred in some tests (7 out of 12 in total) prior to weld rupture.

Representative graphs of the strain distribution around the branch adjacent to the test weld, for various levels of applied load, are given in Figure 7. It is shown that, for 90° connections (Figs. 7a, b), the tensile strain (and hence tensile load) decreases as a function of distance away from the saddle (90° point). The tensile strain is therefore smallest at the crown (0° and 180° points), with much of the weld even remaining in compression for the entire tension load range. This phenomenon equates to a non-uniform loading of the weld perimeter – which is expectedly more pronounced for connections with higher β-values, where stiff membrane action dominates load transfer at the saddle.

The largest tensile strains for 60° connections were initially measured at the saddle (Fig. 7c). As the load increased, the strain adjacent to the saddle,

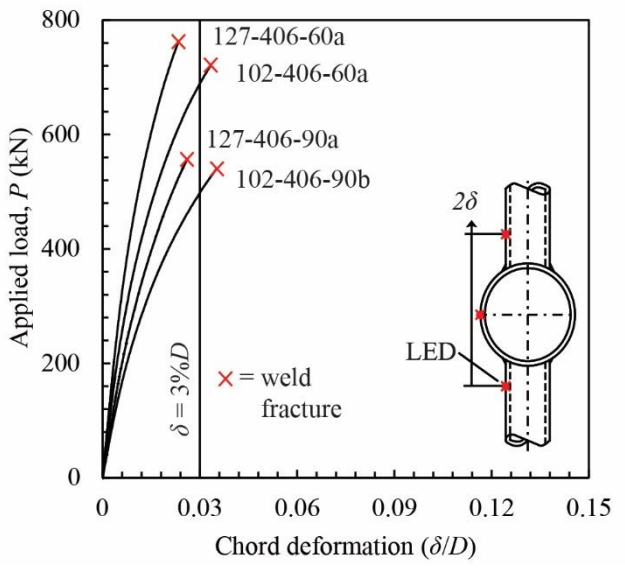

Figure 6. Typical load versus connection displacement relationships.

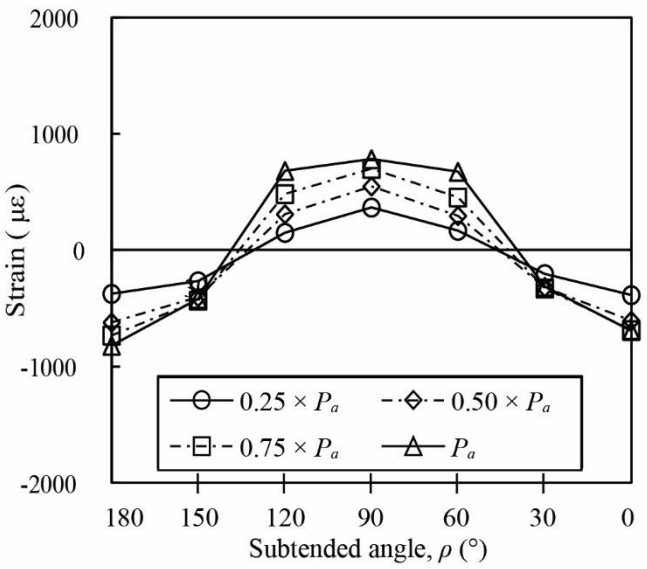

(a) Test no. 127-406-90a (β = 0.31, θ = 90°).

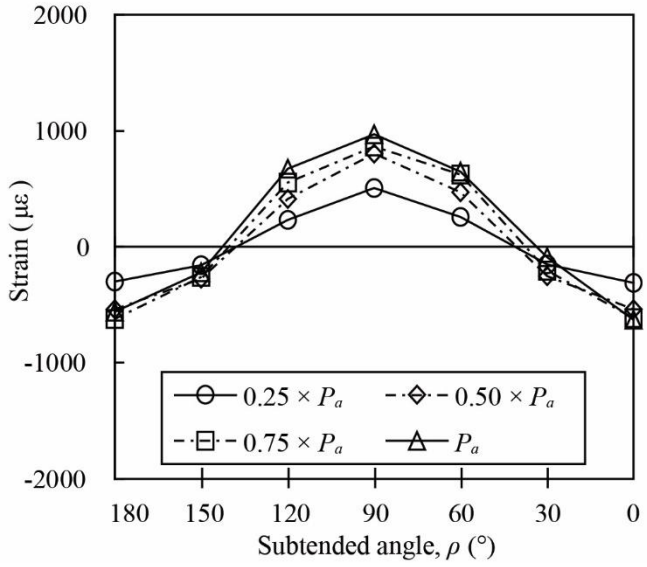

(b) Test no. 127-273-90a (β = 0.47, θ = 90°).

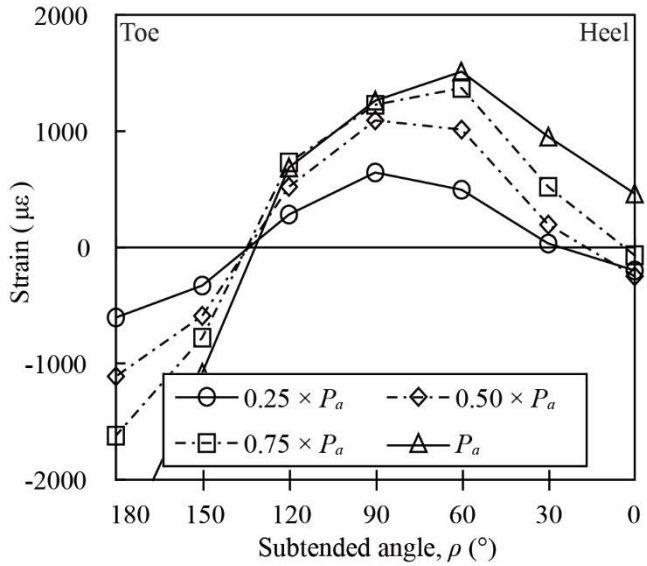

(c) Test no. 102-406-60a (β = 0.25, θ = 60°).

Figure 7. Typical strain distributions adjacent to test weld.

on the heel side of the connection, began to increase at a faster rate than the strain adjacent to the saddle on the toe side of the connection. This is due to secondary bending effects from connection flexibility and joint rotation, which may not exist in real structures where the chord ends are prevented from rotating.

5 EVALUATION OF AWS D1.1-15

5.1 *Existing provisions for weld effective lengths in CHS X-Connections*

According to AWS D1.1-15, the available strength of fillet welds in CHS X-connections designed as "fit-for-purpose" (P_n) is based on the limit state of shear rupture along the plane of the weld effective throat in accordance with Equations 1 and 2 (Clause 9.5.3):

$$P_n = Q_w l_e \tag{1}$$

$$Q_w = 0.60 t_w F_{EXX} \tag{2}$$

where l_e = weld effective length (AWS 2015).

An LRFD resistance factor for fillet welds, ϕ, equal to 0.80, is then applied to determine the design strength.

In Clause 9.5.4, simplified equations are given to compute weld lengths for CHS connections under axial load, which can be traced back to Appendix C of British Standard 449 (BSI 1959). These factors can be shown to calculate the *total* weld length, rather than the *effective* weld length. A branch stress/load factor of 1.50 is specified by AWS, in Clause 9.6.1.3(4), for design using the LRFD method. Thus, the weld effective length implied is the inverse of this factor:

$$l_e = \frac{2}{3} l_w \tag{3}$$

5.2 *Safety level inherent in AWS D1.1-15*

To assess whether adequate or excessive safety margins are inherent, the structural reliability (or safety index) (β^+) can be calculated, and compared to the minimum target value in North America (4.0, as currently adopted by AISC 360-16 per Section B3.1 of the Specification Commentary), using a simplified reliability analysis in which the resistance factor, ϕ, is given by Equation 4 (Ravindra & Galambos 1978, Fisher et al. 1978):

$$\phi = \phi_{\beta+} \rho_R e^{-\alpha_R \beta^+ V_R} \tag{4}$$

where α_R = coefficient of separation taken as 0.55 (Ravindra & Galambos 1978); ρ_R = bias coefficient for resistance (mean ratio of actual-to-predicted weld strength); V_R = associated coefficient of variation (COV) of ρ_R; and $\phi_{\beta+}$ = adjustment factor for β^+ that is needed when $\beta^+ \neq 3.0$ (Fisher et al. 1978). A formula for $\phi_{\beta+}$ was derived by Franchuk et al. (2002):

$$\phi_{\beta+} = 0.0062(\beta^+)^2 - 0.131\beta^+ + 1.338 \tag{5}$$

The mean actual-to-predicted weld strength ratio (ρ_R) was taken as the average over all tests of P_a (Table 1) divided by P_n (Table 2), with P_n calculated using Equations 1, 2 and 3 and the measured values of A_w and F_{EXX}. The reliability analysis parameters, and the results of the reliability analysis, are shown in Table 3.

The implied safety index, β^+, is equal to 8.1 for the existing AWS D1.1 specification provisions, which is much larger than the minimum target safety index of 4.0 in North America. This indicates that a high level of conservatism is present in the AWS D1.1-15 formulae. Figure 8 shows the correlation of the existing AWS D1.1-15 predicted nominal strengths with the experimental results, where upward facing arrows on data point are synonymous with ">" in Table 1. On average, the experimental rupture load is 2.13 times larger than that predicted by AWS.

If, instead, no effective length rules are applied, and the total weld length is used to determine the strength of the welded joint, then the correlation in Figure 9 results. The implied safety index is then 5.2. The mean experimental-to-predicted rupture load is 1.42. As $\beta^+ > 4.0$, it can be concluded that, for the range of parameters studied, weld effective lengths are not required in conjunction with the AWS D1.1 code design method evaluated.

A more rigorous reliability analysis could include typical variations in actual-to-nominal ultimate strength of weld metals. One could also consider variations in the actual-to-predicted weld length, where the predicted weld length could be calculated from the approximation given in AWS D1.1 Clause 9.5.4:

$$l_w = \pi D_b \left(\frac{1 + 1/\sin\theta}{2} \right) \tag{6}$$

Table 3. Reliability analysis parameters.

	AWS D1.1-15		AISC 360-16
l_e / l_w	2/3	unity	unity
ϕ	0.80	0.80	0.75
ρ_R	2.13	1.42	1.42
V_R	0.13	0.13	0.13
$\phi_{\beta+}$	0.68	0.83	0.80
β^+	8.1	5.2	5.6

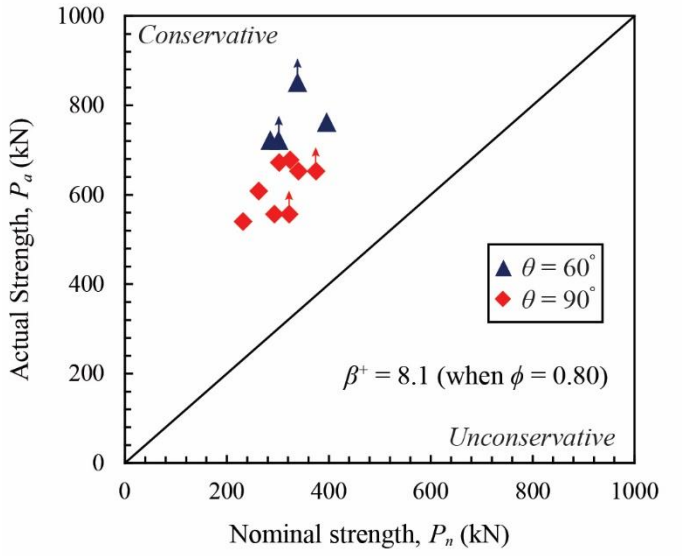

Figure 8. Correlation of existing AWS D1.1-15 provisions with the test results, using weld effective lengths.

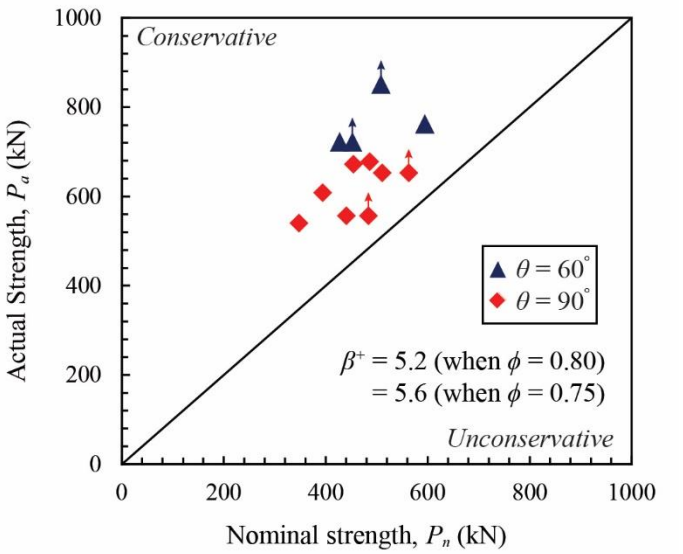

Figure 9. Correlation of AWS D1.1-15 provisions (excluding weld effective lengths) and AISC 360-16 provisions with test results.

Figure 10 shows the relationship between $l_w/\pi D_b$ determined using Equation 6 and $l_w/\pi D_b$ determined from the vector-calculus method, as used herein, for a range of β values. It is shown that Equation 6 is conservative as a design tool (i.e. it under-predicts the weld length). The maximum error is only 1.9% over the range of parameters studied (for β = 0.50 and θ = 90°).

6 COMPARISON TO AISC 360-16

AISC 360-16 gives the same equation (Equation 1) for the available strength of fillet welds via Clause J.2.4a with $l_e = l_w$; however, to calculate the design strength, a resistance factor, ϕ = 0.75 (instead of 0.80), is used. The implied safety index, β^+, is equal to 5.6 for AISC 360-16 Clause J.2.4a (Table 3 and Figure 9), which is expectedly larger than the minimum target safety index of 4.0, and the implied safety index of 5.2 when AWS D1.1 is used without weld effective lengths. The foregoing evaluations of both the AWS and AISC fillet weld design provisions assume that the $(1+0.50\sin^{1.5}\theta)$ directional strength-enhancement factor is not used (AISC 360-16 Clause J2.4b and AWS D1.1-15 Clause 2.6.4.2), because it has been shown to be generally unsafe for the design of fillet welds in HSS connections (Packer et al. 2016).

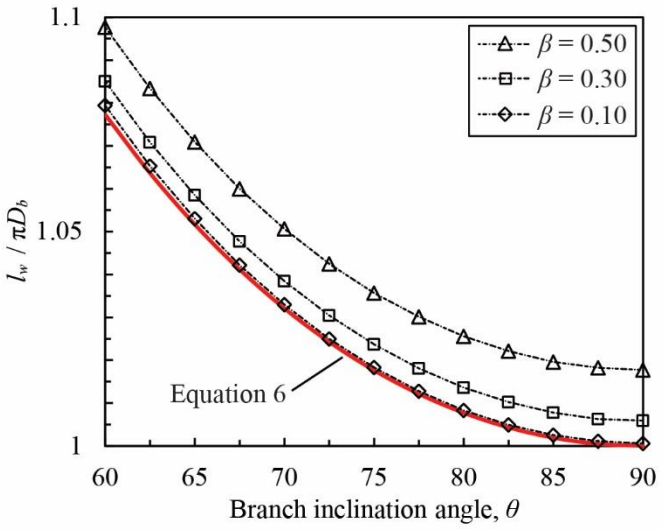

Figure 10. Comparison of $l_w/\pi D_b$ using the AWS D1.1-15 approximation (Equation 6) and the vector-calculus method.

7 CONCLUSION

Based on 12 careful laboratory tests on fillet-welded CHS X-connections, which all failed by rupture along a plane through the weld, it is shown that the existing AWS specification provisions for weld effective lengths (in such connections), given by Clause 9.6.1.3(4), are extremely conservative.

It is shown that both the current AWS and AISC specification provisions provide adequate structural reliability ($\beta^+ \geq 4.0$) without weld effective lengths (i.e. when the total weld length is used to determine the weld strength), assuming the fillet weld directional strength enhancement factor is not used. This is because the analysis method considers the axial force in the branch member to be resisted only by shear stress on the weld throat, which is a conservative assumption.

These conclusions are currently limited to the range of connection parameters studied. A comprehensive parametric modelling study, using finite element methods, and a rigorous reliability analysis are planned, to determine if these findings are applicable to a wider range of fillet-welded CHS X-connections.

ACKNOWLEDGEMENTS

Financial support for this project was provided by the Natural Sciences and Engineering Research Council of Canada (NSERC). CHS sections were donated by Atlas Tube, Harrow, Canada, and in-kind fabrication was provided by Walters Inc., Hamilton Canada. The Authors gratefully acknowledge the laboratory assistance of Mr. Fei Wei.

NOTATION

A_w	weld throat area (= $t_w \times l_w$)
D	diameter of the chord
D_b	diameter of the branch
F_{EXX}	ultimate strength of weld metal
P	applied load
P_a	actual weld fracture load
P_n	nominal predicted weld fracture load
Q_w	shear strength of weld per unit length
V_R	coefficient of variation of ρ_R
l	length of the chord
l_b	length of the branch
l_e	weld effective length
l_h	weld leg along the chord
l_v	weld leg along the branch
l_w	total length of weld
t	thickness of the chord
t_b	thickness of the branch
t_w	weld throat dimension
α_R	coefficient of separation
β	branch-to-chord diameter ratio
β^+	safety index
δ	chord deformation
ρ	subtended angle around the branch, measured clockwise from heel
ρ_R	bias coefficient for resistance
τ	branch-to-chord thickness ratio
ϕ	LRFD resistance factor for fillet welds
$\phi_{\beta+}$	adjustment factor for β^+
θ	branch inclination angle
Ψ	local dihedral angle

REFERENCES

American Institute of Steel Construction (AISC) 2016. ANSI/AISC 360-16. Specification for structural steel buildings. Chicago, IL, USA.

American Welding Society (AWS) 2015. AWS D1.1/D1.1M:2015. Structural Welding Code—Steel. Miami, FL, USA.

ASTM International 2013. ASTM A500-13. Standard specification for cold-formed welded and seamless carbon steel structural tubing in rounds and shapes. West Conshohocken, PA, USA.

ASTM International 2017. ASTM A370-17. Standard test methods and definitions for mechanical testing of steel products. West Conshohocken, PA, USA.

British Standards Institution (BSI) 1959. BS 449:1959. Specification for the use of structural steel in building. London, England.

Fisher, J. W., Galambos, T. V., Kulak, G. L. & Ravindra, M. K. (1978). Load and resistance factor design criteria for connectors. *Journal of the Structural Division, American Society of Civil Engineers* 104(9): 1427-1441.

Franchuk, C. R., Driver, R. G. & Grondin, G.Y. 2002. Block shear failure of coped steel beams. *Proc. Annual Conf. of the Canadian Society for Civil Engineering, Montreal, 5-8 June 2002*.

Frater, G. S. & Packer, J. A. 1992a. Weldment design for RHS truss connections. I: Applications. *Journal of Structural Engineering, American Society of Civil Engineers* 118(10): 2784-2803.

Frater, G. S. & Packer, J. A. 1992b. Weldment design for RHS truss connections. II: Experimentation. *Journal of Structural Engineering, American Society of Civil Engineers* 118(10): 2804-2820.

ISO (International Organization for Standardization). 2013. ISO 14346:2013 (E). Static design procedure for welded hollow section joints – Recommendations, Geneva, Switzerland.

Lu, L. H., de Winkel, G. D., Yu, Y. & Wardenier, J. 1994. Deformation limit for the ultimate strength of hollow section joints. In Paul Grundy, Alan Holgate and Bill Wong (eds.), *Tubular Structures VI; Proc. Intern. Symp., Melbourne 14-16 December 1994*. Rotterdam: Balkema.

Luyties, W. H. & Post, J. W. 1988. Local dihedral angle equations for tubular joints and related applications. *Welding Journal* 77(4): 51-60.

Marshall, P.W. 1992. Design of welded tubular connections – Basis and use of AWS code provisions, Amsterdam, The Netherlands: Elsevier.

McFadden, M. R. & Packer, J. A. 2014. Effective weld properties for hollow structural section T-connections under branch in-plane bending. *Engineering Journal, American Institute of Steel Construction* 51(4): 247-266.

Mehrotra, B. L. & Govil, A. K. 1972. Shear lag analaysis of rectangular full-width tube connections. *Journal of the Structural Division, American Society of Civil Engineers* 98(ST1): 287-305.

Packer, J. A. & Cassidy, C. E. 1995. Effective weld length for HSS T, Y, and X connections. *Journal of Structural Engineering, American Society of Civil Engineers* 121(10): 1402-1408.

Packer, J. A., Choo, Y. S., Shen, W., Wardenier, J., van der Vegte, G. J., & Mustard, T. 2012. CIDECT Report 5BW-2/12. Axially loaded T and X joints of elliptical hollow sections. Geneva, Switzerland: CIDECT.

Packer, J. A., Sun, M., & Tousignant, K. 2016. Experimental evaluation of design procedures for fillet welds to hollow structural sections. *Journal of Structural Engineering, American Society of Civil Engineers* 142(5): 04016007-1 – 04016007-12.

Ravindra, M. K. & Galambos, T. V. 1978. Load and resistance factor design for steel. *Journal of the Structural Division. American Society of Civil Engineers* 104(9): 1337-1353.

Tousignant, K. & Packer, J. A. 2015. Weld effective lengths for rectangular HSS overlapped K-connections. *Engineering Journal, American Institute of Steel Construction* 52(4): 259-282.

Tousignant, K. & Packer, J. A. 2016. Experimental evaluation of directional strength-enhancement factor for fillet welds to CHS. *Connections VIII; Proc. Intern. Workshop on Connections in Steel Structures, Boston, 24-25 May 2016*.

van der Vegte, G.J. & Makino, Y. 2010. Further research on chord length and boundary conditions of CHS T- and X-joints. *Advanced Steel Construction* 6(3): 879-890.